Journal of Hazardous Materials 424 (2022) 127590

Contents lists available at ScienceDirect

Journal of Hazardous Materials

journal homepage: www.elsevier.com/locate/jhazmat

Research Paper

Variations of significant contribution regions of NO_x and PN emissions for passenger cars in the real-world driving

Jianbing Gao [a,*], Yufeng Wang [a], Haibo Chen [b], Juhani Laurikko [c], Ye Liu [b], Ari-Pekka Pellikka [c], Ying Li [d]

[a] School of Mechanical Engineering, Beijing Institute of Technology, Beijing 100081, China
[b] Institute for Transport Studies, University of Leeds, Leeds LS2 9JT, UK
[c] Engine and Vehicle Emissions, VTT, 02044 VTT, Finland
[d] Dynnoteq, 61 Bridge Street, Kington HR5 3DJ, UK

ARTICLE INFO

Editor: Dr. R Teresa

Keywords:
Real-world driving
NO_x
Particle number
Emission contribution regions
Driving behaviors

ABSTRACT

Nitrogen oxides (NO_x) and particulate number (PN) emissions are the main concerns of the passenger cars in the real-world driving. NO_x and PN emissions are greatly dependent on the driving behaviors which differ significantly between standard driving cycles and real-world driving. However, the significant contribution regions (short durations corresponding to high proportions of total emissions) of NO_x and PN emissions regarding different driving behaviors (e.g. vehicle speed and acceleration) are still uncovered. $NO_{x20\%}$ and $NO_{x50\%}$ refer to instantaneous NO_x emission rates when NO_x emission rates are ranked from high to low level where the sums of NO_x emission rates being higher than $NO_{x20\%}$ and $NO_{x50\%}$ correspond to 20% and 50% of total NO_x emissions, respectively. $t_{20\%}$ and $t_{50\%}$ are corresponding durations where NO_x emission rates are higher than $NO_{x20\%}$ and $NO_{x50\%}$. In this paper, three Euro-6 compliant direct injection gasoline passenger cars and a diesel passenger car are tested in a real-world driving trial in which nineteen drivers are involved. Novel key performance indicators with reference to the regimes of specific NO_x and PN contributions to total emissions are defined. Instantaneous NO_x and PN emissions are monitored using a portable emission measurement system (PEMS) in the test. The results indicate that the maximum and minimum average speed over the four cars being approximately 32.3 km/h s and 42.6 km/h, respectively. Average PN emission factor of the diesel car is the lowest among the four given cars. Average $t_{20\%}$ and $t_{50\%}$ corresponding to $NO_{x20\%}$ and $NO_{x50\%}$ are lower than 3% and 12%, respectively, for all the passenger cars; additionally, these two parameters show the same pattern. The corresponding $t_{20\%}$ and $t_{50\%}$ variations of the Euro-6a gasoline car and the diesel car are much lower than the other two. Average acceleration corresponding to 20% and 50% of total NO_x emissions for the given diesel car is approximately 1.25 m/s^2 and 0.6 m/s^2, respectively, being much higher than that of the other three gasoline cars (lower than 1 m/s^2 and 0.4 m/s^2 respectively) over the specific driving route and drivers. The average $PN_{20\%}$ and $PN_{50\%}$ of the given diesel car are approximately 7×10^7#/s and 3×10^7#/s respectively, being much lower than the three given gasoline cars (higher than 8 $\times 10^9$#/s and 2 $\times 10^9$#/s respectively) under the given test conditions; the corresponding $t_{20\%}$ and $t_{50\%}$ are lower than 4% and 17% respectively for all the three gasoline cars.

1. Introduction

Exhaust emissions from on-road vehicles have significant negative impacted environment and human health (Gao et al., 2022; Tong et al., 2020). Carbon monoxide (CO), hydrocarbon (HC), nitrogen oxides (NO_x), and particles are the regulated pollutants from on-road vehicles (Nagpure et al., 2016; Wang et al., 2017b; Wu et al., 2017). In order to decrease the exhaust emissions, stricter emission regulations and test procedures are adopted (Carslaw et al., 2011). Particles are easy to be inhaled into the respiratory systems due to their small size (Penconek et al., 2013). The Euro-6 emission standard not only limits particulate mass emission but also particulate number (PN) emission (Weber et al., 2019; Yinhui et al., 2016). According to the UK government report published in 2019 (The UK Government, 2021), PM10 (i.e. particles smaller than 10 μm in diameter), PM2.5 (i.e. particles smaller than 2.5 μm in diameter), and NO_x emissions from road transport account for approximately 12%, 13%, and 33% of the country's total emissions,

* Corresponding author.
E-mail addresses: gaojianbing@bit.edu.cn, redonggaojianbing@163.com (J. Gao).

https://doi.org/10.1016/j.jhazmat.2021.127590
Received 20 August 2021; Received in revised form 20 October 2021; Accepted 21 October 2021
Available online 27 October 2021
0304-3894/

Nomenclature

CNG	compressed natural gas
CO	carbon monoxide
DOC	diesel oxidation catalyst
DPF	diesel particulate filter
EFM	exhaust flow meter
GDI	gasoline direct injection
GPF	gasoline particulate filter
GPS	global positioning system
HC	hydrocarbon
KPIs	key performance indicators
LNT	lean NO_x trap
NEDC	New European Driving Cycle
NO_x	nitrogen oxides
PEMS	portable emission measurement system
PM	particulate matter
PN	particulate number
RDE	real-world emissions
SCR	selective catalytic reduction
TWC	three way catalyst
UK	United Kingdom
UV	ultraviolet
WLTC	Worldwide Harmonized Light Vehicles Test Cycle

respectively. The main issues of the exhaust emission reductions are NO_x and particles (especially PN) (Carslaw et al., 2011). NO_x and particle emissions are significantly dependent on driving behaviors and after-treatment efficiency. NO_x after-treatment systems such as selective catalytic reduction (SCR) are usually the farthest from the engine, operating at relative low temperature, compared to other after-treatment devices. This configuration often leads to low NO_x reduction efficiency, especially under unfavorable vehicle operation conditions such as low vehicle speed or small acceleration (Gao et al., 2021b). Diesel particulate filter (DPF) and gasoline particulate filter (GPF), as the most successful particle removal devices, present high particulate matter (PM) removal efficiency; however, it is less effective to decrease ultra-fine particles (Guan et al., 2015). It results in low PM pipe-out emission, but the PN emission is still high. Driving behaviors affect both emission formations and catalyst-based after-treatment efficiency (Gao et al., 2021b).

Driving behaviors in real-world are much more complex than standard driving cycles. Real-world driving usually has sharper and more frequent acceleration events (Pathak et al., 2016). It was widely reported that the real-world driving emissions were much higher than that of the standard driving cycles (Fontaras et al., 2009; Gao et al., 2019a, 2019b; Valverde et al., 2019). CO, HC, and NO_x emissions over real-world driving were reported to be approximately 155%, 63%, and 64% higher than Worldwide Harmonized Light Vehicles Test Cycle (WLTC) respectively for light gasoline passenger cars (Pathak et al., 2016). The real-world NO_x emission factors of diesel cars were demonstrated to be much higher than that of gasoline cars (O'Driscoll et al., 2018), concluded by an experiment of 149 Euro-5 and Euro-6 passenger cars. The NO_x emission factors of Euro-5 and Euro-6 passenger cars in urban area presented approximately 300% and 400% higher than their corresponding emission limits. It was proved that average NO_x emission factors of three diesel passenger cars over real-world driving were approximately 2 g/km which was approximately three times and ten times of the emission factors over WLTC and New European Driving Cycle (NEDC) respectively (Triantafyllopoulos et al., 2019); additionally, the NO_x emission factors of diesel cars under real-world driving conditions were demonstrated to be approximately eight times higher than NEDC in the work (Degraeuwe and Weiss, 2017). However, NO_x emission factors (33 mg/km) of a specific gasoline car under real-world driving were below the Euro-5 emission standard limits although they were still approximately 80% higher than the factors under NEDC conditions (Degraeuwe and Weiss, 2017). It was considered to be mainly caused by gentle driving under the real-world driving conditions.

PN emission is determined by combustion conditions and particle evolutions which significantly affect particle phases. Factors such as the engine thermal status, tailpipe temperature, and atmosphere temperature are very important to form liquid-phase particles which accounted for a high proportion under specific conditions (Liu et al., 2021). It was demonstrated that liquid-phase particles accounted for approximately 94% of the total particles in number when the atmosphere temperature was below 0 °C (Wang et al., 2017a); the percentage was dropped to 85% for 20 °C ambient temperature. PN emission from gasoline, diesel, and compressed natural gas (CNG) light duty vehicles under real-world driving conditions (Kontses et al., 2020). The Euro-6 diesel vehicle (with DPF) and the CNG vehicle showed the lowest PN emission; direct injection gasoline vehicles without GPF had the highest PN emission factors. PN emission factors of the Euro-6b gasoline vehicles without GPF reached 1.3×10^{13}#/km; however, they were lower than 3.1×10^{10}#/km for the diesel vehicles with DPF (Kontses et al., 2020). Engine warm status presented significant impacts on PN emission factors (Zhang et al., 2021). PN emission factors including cold start stages were three times higher than hot start real-world driving (Kontses et al., 2020). Additionally, the liquid-phase particles were tended to be smaller than solid-phase particles. It was also showed that PN emission factors were approximately 2×10^{12}#/km for a Euro-6b GDI car without GPF under the real-world driving, and the emission factors were below 9×10^{11}#/km under the assistant of GPF (Demuynck et al., 2017).

NO_x and PN emissions were demonstrated to be closely related to driving behaviors for passenger cars (Gao et al., 2021b; Ramos et al., 2018). High emission rates mainly happened in low vehicle speed and high acceleration regimes (Gao et al., 2021b). The effects of driving behaviors on pipe-out NO_x and PN emissions included the impacts from NO_x and PN formations and after-treatment system efficiency. The secondary particle formations, mainly caused by condensations of HC in the tailpipe were also a vital factor influencing the relationships between driving behaviors and PN emissions. The differences of NO_x emissions caused by driving behavior variations were up to 55% (Varella et al., 2019); the cold-operation increased NO_x emissions by approximately 55% compared to hot-operation. Driving behaviors affected the exhaust temperature, further generating the impacts on catalyst efficiency (Gao et al., 2021b). Acceleration at low speed of a Euro-6 light-duty diesel vehicle led to higher NO_x emissions than constant high speed (Luján et al., 2018).

High acceleration and low catalyst temperature were the main factors leading to NO_x emission peaks which were much higher than normal emission rates. It was reported that the instantaneous NO_x emissions of passenger cars with SCR and lean NO_x trap (LNT) devices (Mera et al., 2019). The NO_x peaks under both SCR and LNT conditions reached 220 ppm, being ten times higher than of normal values. NO_x and particle emission peaks were usually observed in the acceleration events. It was observed that high NO_x emission peaks in the aggressive acceleration process, being higher than 0.04 g/s for a diesel cars under real-world driving (Luján et al., 2018). The peaks of the particle emission rates during acceleration were demonstrated to be hundreds times higher than normal driving conditions (Wang et al., 2020). Similar phenomenon was also observed in the work (Myung et al., 2020) based on a real-world driving where a gasoline direct injection passenger car was fuelled with different types of fuels. It addressed the significant contributions of high emission peaks to the total emissions.

As mentioned above, there are some regimes where the emission

Table 1
Vehicle specifications of the test cars.

Car label		Car-A	Car-B	Car-C	Car-D
Car maker		Ford	Opel	Skoda	Skoda
Model		Feista	Crossland-X	Octavia	Octavia
Manufacture year		2015	2019	2017	2019
Fuel type		Gasoline	Gasoline	Gasoline	Diesel
Fuel delivery		Direct injection	Direct injection	Direct injection	Direct injection
Aspiration		Turbocharged	Turbocharged	Turbocharged	Turbocharged
Engine size/ L		1.0	1.2	1.5	1.6
Max. power/ kW		73.5	81	110	85
Compression ratio		10.0	10.5	12.5	16.2
Running mass/ kg		1100	1320	1470	1556
After-treatment	Gaseous	Three way catalyst (TWC)	TWC	TWC	DOC+SCR
	Particles	N.A.	GPF	N.A.	DPF
Emission standards		Euro-6a	Euro-6d	Euro-6c	Euro-6d
Gear number (type)		5 (M)	5 (A)	6 (M)	7 (DSG)
Type approval cycle		NEDC	WLTP	WLTC	WLTC
Type approval NO_x (mg/km)		40	17.5	34.1	29.2
Type approval PN (10^{11} #)		N.A.	4.2	1.08	0.02
Type approval CO_2 (g/km)		99	153	115	141

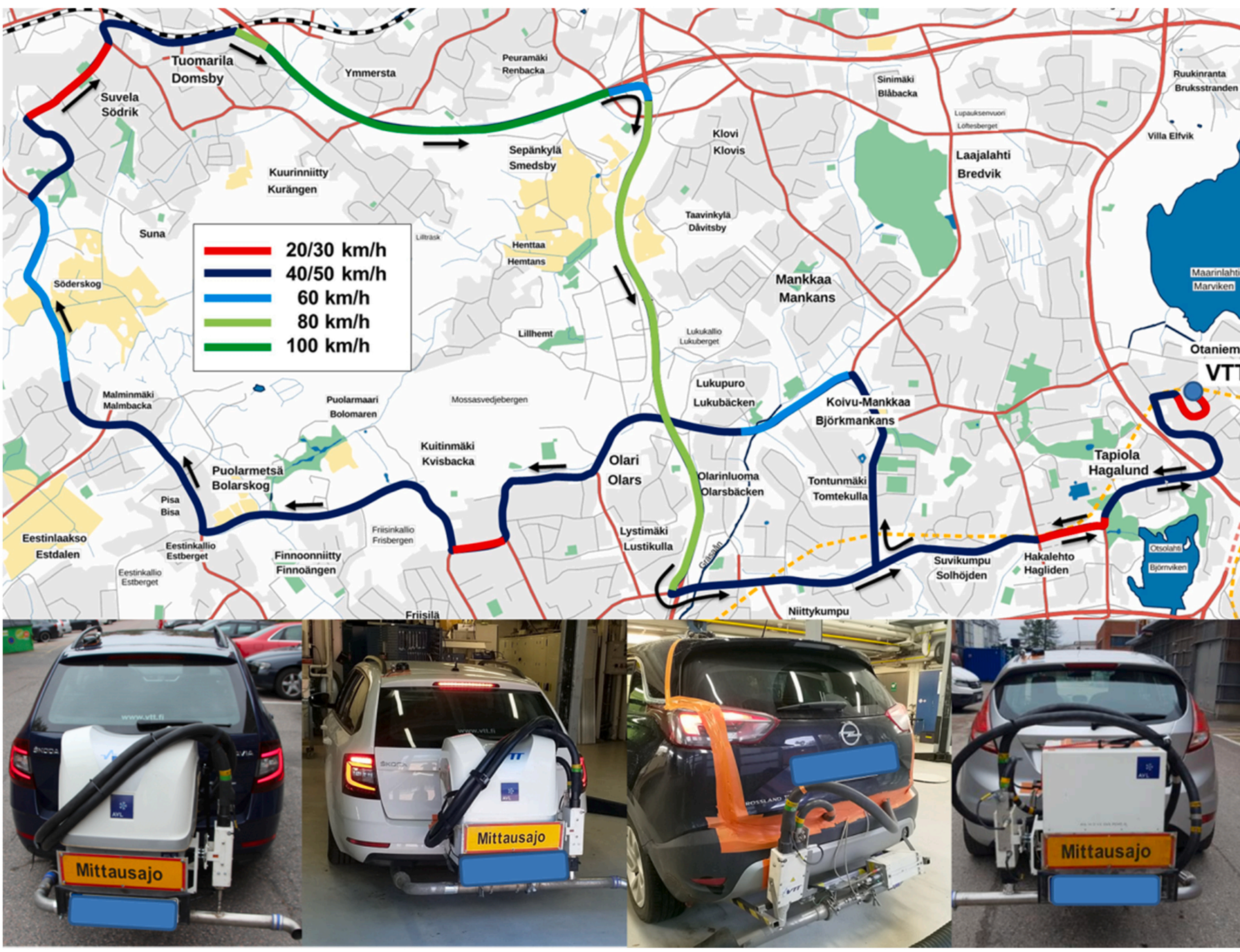

Fig. 1. Real-driving test routes of the passenger cars.

rates were much higher than normal driving and contribute a significant proportion of the total emissions in the real-world driving. The significant contribution regimes are the operation conditions where the measures can be taken to further decrease the emissions. However, the significant contribution regimes have not been investigated under real-world driving conditions for passenger cars to the authors' knowledge; additionally, the variations of such regimes over different drivers are still unknown. In this paper, the key performance indicators (KPIs) evaluating the contributions of high emission peaks, high vehicle acceleration, and high vehicle speed regions to the total NO_x and PN emissions in the real-world driving are put forward. Further, the variations of the KPIs among nineteen drivers are analyzed. The differences of

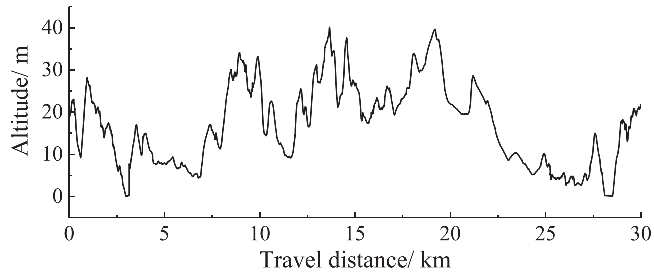

Fig. 2. Altitudes along the journey.

the statistical results among three given gasoline cars and a given diesel car are discussed.

2. Experimental section

In this section, the specifications of the passenger cars in the test are presented; additionally, test equipment and procedures are shown; KPIs evaluating specific contributions to total emissions are defined as well.

2.1. Vehicle information

In this work, four vehicles including three gasoline cars and one diesel car are used to perform the real-world emission test. The specifications of the four cars are shown in Table 1. They meet Euro-6 emission standard but over different approval test cycles and test procedures; additionally, they have direct fuel injection system but different after-treatment systems. Euro-6 emission regulation limits PN emission for both direct injection vehicles and diesel vehicles. Regarding gasoline cars, direct fuel injection systems generate much more particles than port fuel injection systems. In Euro-6d emission regulation, GPFs are necessary to control particle emissions from direct injection gasoline cars. As shown in Table 1, type approval NO_x emissions of Euro-6a cars are much higher than those of Euro-6c and Euro-6d counterparts.

2.2. Test equipment and procedures

The real-world test was conducted in the city of Helsinki, Finland, as shown in Fig. 1. The test route starts and ends at the VTT campus, including rural roads, urban roads, and motorways, comprising 76.8%, 16.5%, and 6.7% of the total distance, respectively (Gao et al., 2021a). Speed limits of the road segments are also marked in the figure. During the test, the altitudes of the test road were recorded, as presented in Fig. 2. There is not any congestion during the test.

Real-world emissions of exhaust pollutants such as NO_x and PN from the four cars were monitored using a state-of-the-art gas PEMS (AVL M.O.V.E PEMS) and a particle PEMS. The systems include a gas module and a particle module which accurately measure the instantaneous NO_x and PN emission rates (1 Hz). An ultraviolet (UV) analyser was used to measure NO_x emissions. Only the solid-phase particles being larger than 23 nm were counted by the PEMS systems. The thermal denuder embedded in the system was heated to 300 ℃ to avoid the impacts from high-volatility organic compounds and water vapors. Both PEMS systems were installed at the back of the cars (or in the cars), and an extension to the exhaust tailpipe was used to mount an exhaust flow meter (EFM) tube along with a sensor used to monitor exhaust flow rates and temperature, as well as a sampling probe at the end. Fig. 1 is the example of an installation. The PEMS systems were calibrated before the test, and the cars were fully warmed up before the test to avoid the cold-start effect. A post-processing program was used to record the sampling data, including gaseous pollutants and PN. The trajectories of the vehicle including longitude, latitude, and altitude were also recorded by a global positioning system (GPS). In this paper, the analysis was only

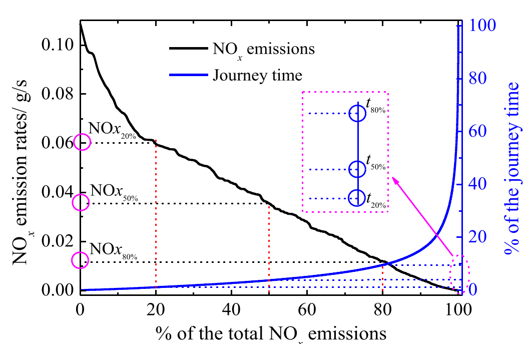

(a) NO_x emission rates, % of the journey time *vs*. % of the total NO_x emissions

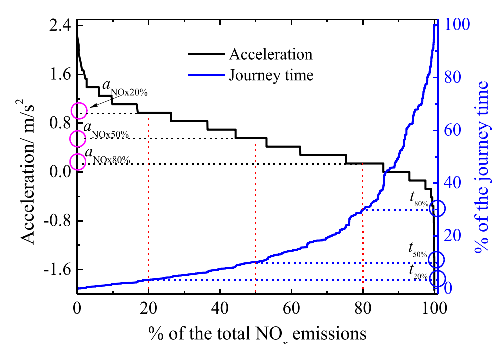

(b) Acceleration, % of the journey time *vs*. % of the total NO_x emissions

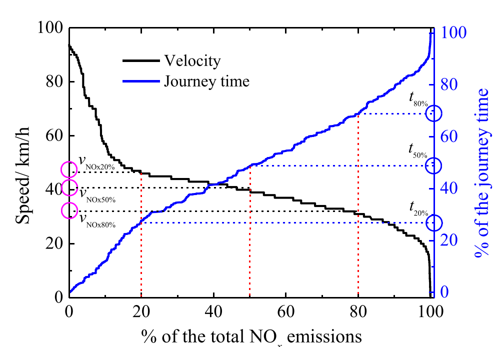

(c) Speed, % of the journey time *vs*. % of the total NO_x emissions

Fig. 3. NO_x emission rates, acceleration, and speed related parameters.

Table 2
Key performance indicator definitions.

KPIs	Definitions (based on the profiles inFig. 3)	Corresponding travel durations
$NO_{x20\%}$	NO_x emission rates corresponding to 20% of the total NO_x emissions	$t_{20\%}$
$a_{NOx20\%}$	Acceleration corresponding to 20% of the total NO_x emissions	
$v_{NOx20\%}$	Speed corresponding to 20% of the total NO_x emissions	
$PN_{20\%}$	PN emission rates corresponding to 20% of the total PN emissions	
$a_{PN20\%}$	Acceleration corresponding to 20% of the total PN emissions	
$v_{PN20\%}$	Speed corresponding to 20% of the total PN emissions	
$NO_{x50\%}$	NO_x emission rates corresponding to 50% of the total NO_x emissions	$t_{50\%}$
$a_{NOx50\%}$	Acceleration corresponding to 50% of the total NO_x emissions	
$v_{NOx50\%}$	Speed corresponding to 50% of the total NO_x emissions	
$PN_{50\%}$	PN emission rates corresponding to 50% of the total PN emissions	
$a_{PN50\%}$	Acceleration corresponding to 50% of the total PN emissions	
$v_{PN50\%}$	Speed corresponding to 50% of the total PN emissions	

focused on NO_x and PN emissions which are the main concerns of the modern passenger cars.

2.3. Parameter definitions

In this section, the key performance indicators evaluating the regimes of the specific contributions to total emissions are defined in terms of driving behaviors. As demonstrated by the work (Luján et al., 2018; Mera et al., 2019; Suarez-Bertoa et al., 2019b), the majorities of NO_x and PN emissions are contributed by a small part of driving events. For example, peak NO_x emission rates are more than 10 times higher than that of normal driving (Mera et al., 2019); peak PN emission rates caused by aggressive acceleration events are hundreds times higher than that of gentler driving (Myung et al., 2020). These driving events may be an opportunity in which the driving behaviors can be improved to achieve low emissions. Fig. 3 shows the percentage of the journey time, NO_x emission rates, acceleration, and speed profiles against the percentage of the total NO_x emissions. Similar figures related to PN emission are also provided in Fig. S1. When analyzing real-world test data, the authors found that KPIs corresponding to 20% of total emissions were contributed by aggressive events around such as the traffic lights and road corners; in addition, KPIs corresponding to 50% of the total emissions reflect the overall driving behavior level related to real-world emissions. Additionally, the specific definitions of the KPIs in this paper are provided in Table 2.

3. Results

In this section, a matrix of nineteen drivers and 4 passenger cars is created to test their real-world driving emissions. Firstly, the variations of real-world driving behaviors and emission factors of nineteen drivers are analyzed; then, the KPIs relating to specific contributions of NO_x and PN emissions to total emissions from the viewpoint of driving behaviors are discussed.

3.1. Variations of the travel characteristics over different drivers

Driving behaviors vary greatly from driver to driver even on the

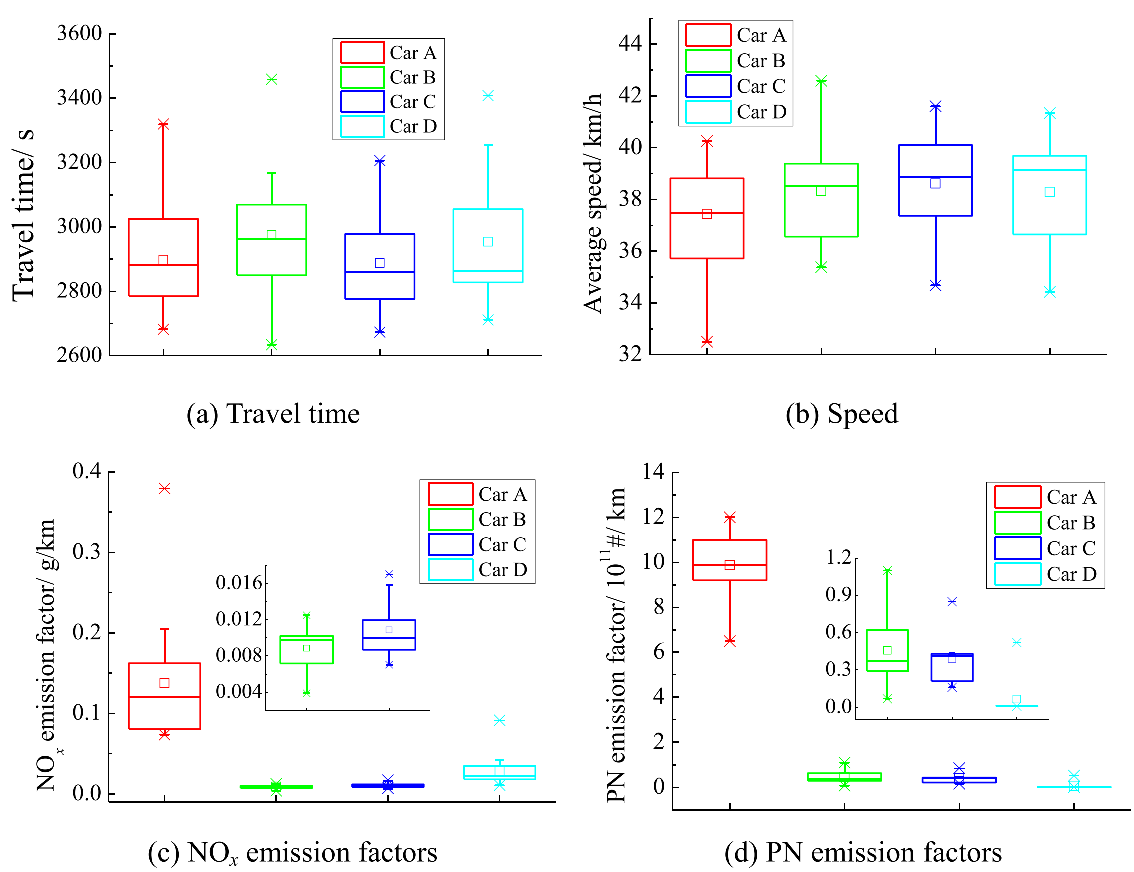

Fig. 4. Travel characteristics over the matrix of nineteen drivers and four cars.

Table 3
Ratios of real-world emissions to those over standard driving cycle.

Emissions	NO_x				PN			
Ratio	Car-A 2.29	Car-B 0.15	Car-C 0.18	Car-D 0.35	Car-A 1.65*	Car-B 0.11	Car-C 0.36	Car-D 3.22

* Type approval value is not available, so the Euro 6 PN limit is used.

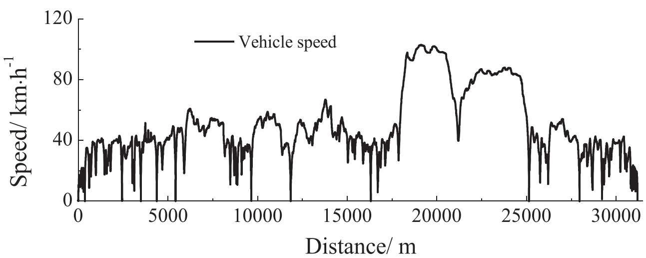

Fig. 5. A typical speed profile during the test.

same route and under similar traffic conditions. Fig. 4 shows the travel characteristic variations among nineteen drivers, including travel time, average speed, NO_x emission factors, and PN emission factors. The explanations of the bars and lines in box plots are presented in the work (Li, 2019). The differences of average travel time and average speed were small between different types of passenger cars; the maximum difference of travel time was higher than 35%. However, the variations of travel time and speed of different drivers with the same car were large. The average speed was approximately 37.4 km/h, 38.4 km/h, 38.8 km/h, and 38.4 km/h for Car-A, Car-B, Car-C, and Car-D, respectively. Average NO_x and PN emission factors of Car-A were much higher than others, with the average value being approximately 0.14 g/km and 9.9×10^{11}#/km, respectively. It was indicated by the work (Kadijk et al., 2017), NO_x emission factors of six passenger cars meeting Euro-5 and −6 emission regulations were in the range of 0.05 g/km~2 g/km in the real-world driving although majority of the vehicles complied in type approval emission tests. Variations of NO_x emission factors from high emission cars were demonstrated to be much higher than those of low emission cars (Hu et al., 2012). It was consistent with the authors' test results. The PN emission factor was lower than Euro-6 emission limits even without GPF, being mainly resulted from the test procedure in this paper where the cars were fully warmed up. Car-A met Euro-6a emission regulation where the approval test procedure was based on NEDC, resulting in higher NO_x emission factor than limits. NEDC test procedure was gentler than WLTC, partly leading to high emission factors of Euro-6a compliant cars under real-world driving conditions. Car-A was a direct injection engine, and was free of GPF. Regarding PN emission from the given direct injection gasoline cars in this paper, the emission level was the same or even higher than the given diesel car. The test results agreed with the work (Kontses et al., 2020), indicating that Euro-6 diesel cars equipped with DPF showed lower PN emission factors than Euro-6 gasoline cars without GPF under real-world driving conditions. PN emission factors of Euro-6 gasoline cars without GPF reached 1.3×10^{13}#/km (Kontses et al., 2020). Regarding the two Euro-6d passenger cars (Car-B and Car-D), average NO_x emission factors of the diesel passenger car (Car-D) were higher than the gasoline passenger car (Car-B); however, the average PN emission factors of the diesel car (Car-D) were much lower than that of the given gasoline cars. Even though the direct injection gasoline passenger car (Car-B) was equipped with GPF, it was still much more difficult to control PN emission than the diesel passenger car.

Ratios of real-world emissions to those over standard driving cycle are shown in Table 3; in the meantime, a typical speed profile during the test is provided in Fig. 5. Regarding the ratios of NO_x emissions, Car-A showed the highest value, and they were lower than 0.4 for the other

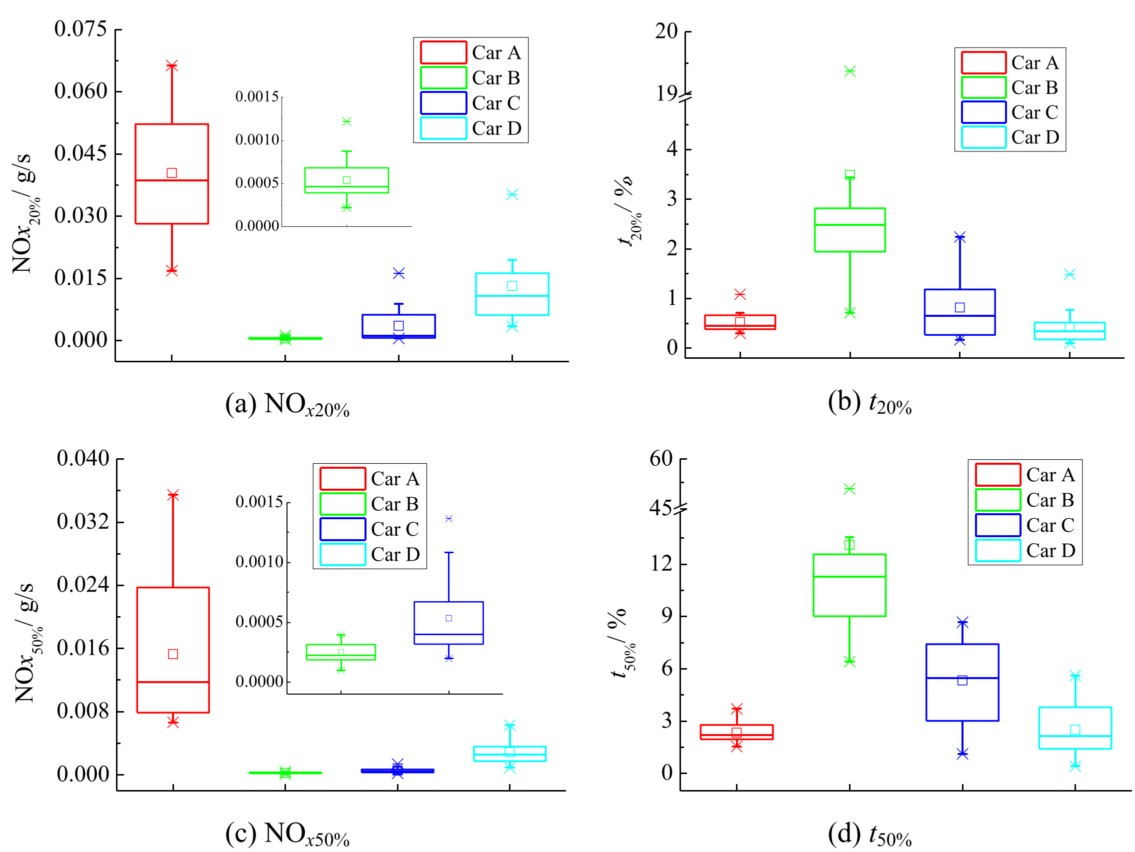

Fig. 6. NO_x emission rates and corresponding durations over 20% and 50% of the total NO_x emissions.

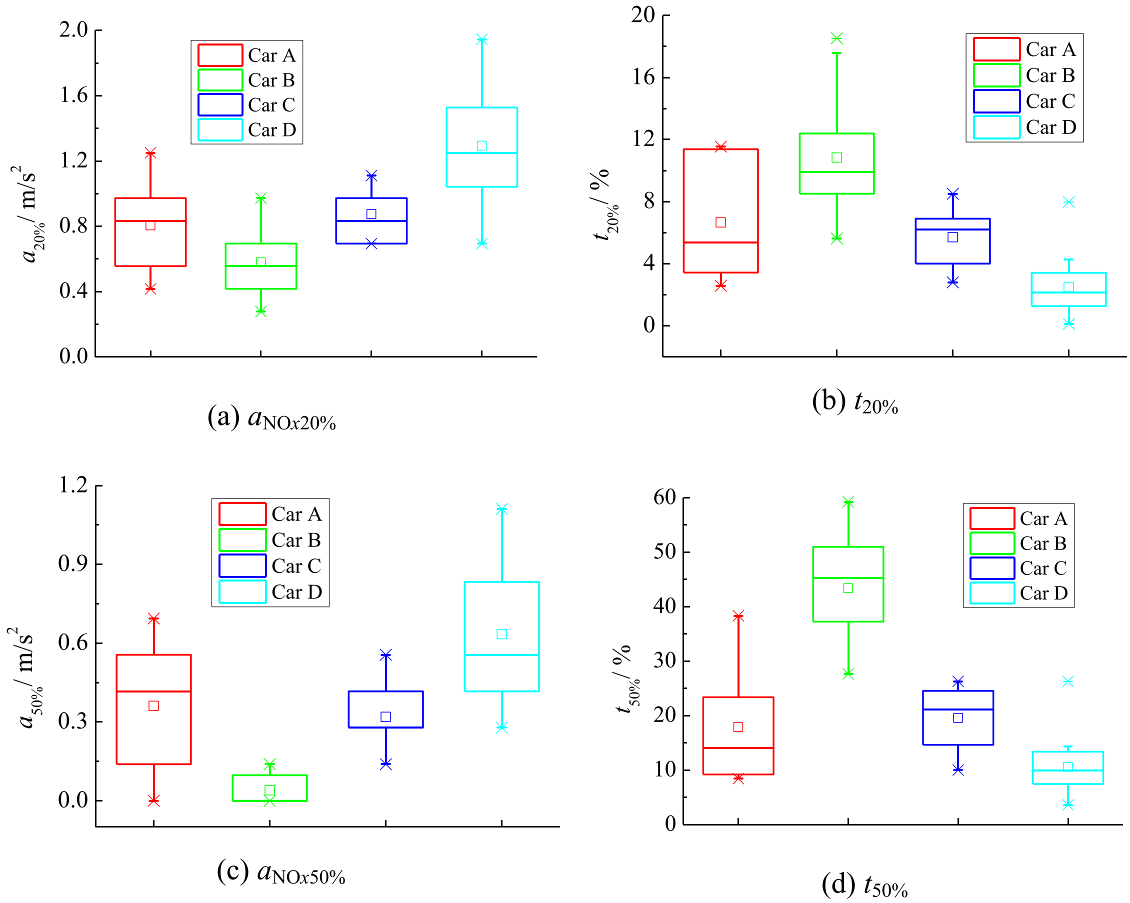

Fig. 7. Acceleration and corresponding durations over 20% and 50% of the total NO_x emissions.

three cars. The ratios of PN emission were 1.65, 0.11, 0.36, and 3.22 for Car-A, Car-B, Car-C, and Car-D, respectively. The ratio of the Car-D (diesel car) was much higher than the type approval value although it was equipped with a DPF. The ratio was higher than 1 if the real-world driving cycle was complied with the standard test procedure, as demonstrated by previous published work (Triantafyllopoulos et al., 2019). It was demonstrated that the real-world NO_x emission factors were on average 5–6 times higher than the type approval limits for Euro-5 and −6 diesel cars (Kadijk et al., 2017). Table 3 also presented a typical speed profile of the four cars over different drivers. The speed profile was significantly different from WLTC driving cycle, with relative fewer aggressive driving events, lower maximum speed, and lower average speed. Additionally, the passenger cars were fully warmed up before the test to exclude the effect of cold start on the relationship between driving behaviors and emissions. It was approved that most of the NO_x emissions were generated during the warm up process (Gao et al., 2019b); in the meantime, a significant amount of the liquid-phase particles were formed under the low exhaust temperature conditions (Huang et al., 2013). The research (Kontses et al., 2020) also proved that PN emission factors over cold-start real-world driving reached 1.2×10^{12} #/km which was approximately twelve times of hot real-world driving conditions for a Euro-6b GDI car. The fact addressed the importance of the cold-start effect on PN emission factors of GDI cars. During the test in the authors' paper, only the solid-phase particles (soot) were counted, as mentioned in Section 2. These factors led to the low values of PN emission ratios in Table 3. The result was consistent with a previous published paper where NO_x emission factors of a gasoline car under real-world driving was lower than those over NEDC conditions (Degraeuwe and Weiss, 2017). It was mainly caused by the fact that the driving behaviors under real-world driving conditions were gentler than those of NEDC.

3.2. Variations of NO_x related KPIs

The NO_x reduction efficiency of three way catalyst (TWC) and SCR significantly depended on the exhaust temperature (Merkisz et al., 2019); additionally, many liquid-phase particles were formed in the tailpipe under the cold atmosphere conditions (Drozd et al., 2018). As a result, cold start events would affect the analysis of drivers' impacts on exhaust emission factors (Gao et al., 2019a, 2019b). The passenger cars were fully warmed up before the test to exclude the effect from cold start. High emission regimes usually have a significant contribution to the total emissions and account for a small proportion of total travel time. Fig. 6 shows the variations of NO_x emission rates and corresponding durations of $NO_{x20\%}$ and $NO_{x50\%}$. Average $NO_{x20\%}$ was approximately 0.038 g/s for Car-A, and the corresponding $t_{20\%}$ was lower than 1%; meantime, the variations of NO_x emission rates from Car-A were the highest among the four cars. It implied that very short operation durations led to much high NO_x emissions. The research (Mera et al., 2019) also indicated that high instantaneous NO_x represented a small percentage of observations or driving duration but a large percentage of total NO_x emissions. 1.6% of the total driving duration contributed 20% of total NO_x emissions for the car with LNT after-treatment, and the duration was dropped to 0.7% for SCR scenarios. $NO_{x20\%}$ was approximately 66.2 mg/s and 21.3 mg/s for the Euro-6b diesel cars equipped with LNT and SCR, respectively (Mera et al., 2019), and the value was higher than the authors' results. Driving behaviors of the Car-A drivers seemed to affect the real-world NO_x emissions greater than other cars. Large variations in average $NO_{x20\%}$ meant high possibilities of high emission rate points during driving.

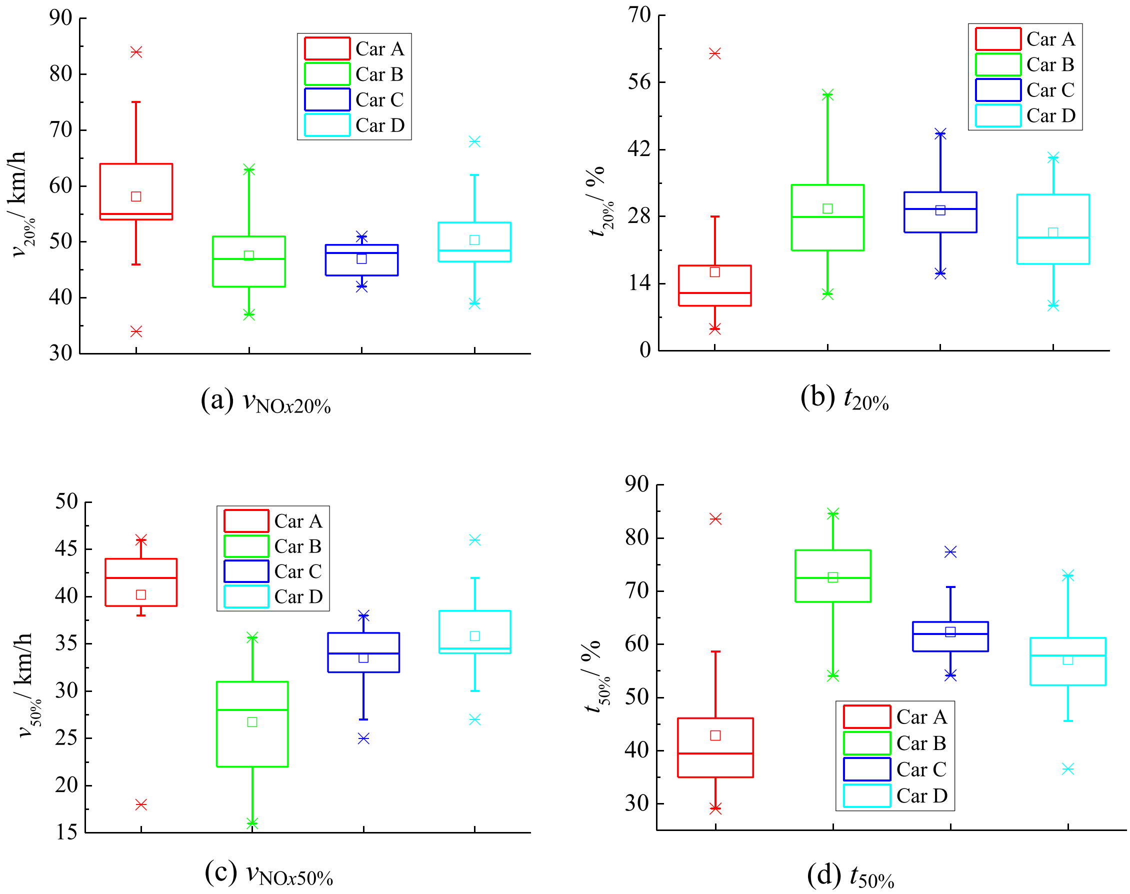

Fig. 8. Vehicle speed and corresponding durations over 20% and 50% of the total NO_x emissions.

Average $NO_{x20\%}$ of Car-B was the lowest, being approximately 0.0005 g/s. $NO_{x20\%}$ variations of Car-B were much smaller than the other cars; however, the variations of corresponding $t_{20\%}$ were the biggest. For the Euro-6d compliant cars in the test (Car-B and Car-D), the average $NO_{x20\%}$ of the diesel car (Car-D) was higher and its $t_{20\%}$ was lower than that of the gasoline car (Car-B). Average $t_{20\%}$ corresponding to $NO_{x20\%}$ was the lowest for the diesel car, indicating that high NO_x emission peaks were more important to total emissions for diesel cars than to the gasoline counterparts. The analysis also showed that $NO_{x20\%}$ had an opposite tendency with corresponding $t_{20\%}$; high emission cars tended to present small value of average $t_{20\%}$. Lower NO_x emission cars had fewer NO_x emission peaks. Average $t_{20\%}$ corresponding to $NO_{x20\%}$ was smaller than 3.5% for all the cars in the test. It emphasized the importance of high emission regimes. Variations of NO_x emission factors for a diesel car were quite low because the driving speed profile in the test was controllable (given in the lab); in addition, low average NO_x emission fuel categories tended to have low variations (Suarez-Bertoa et al., 2019a). It had been demonstrated that NO_x emission variations of Euro-6 diesel cars were slightly higher than those of Euro-6 gasoline cars. It implied the high possibility of high emission factors for diesel cars under real-world driving conditions.

$NO_{x50\%}$ and corresponding $t_{50\%}$ had a similar tendency to $NO_{x20\%}$ and corresponding $t_{20\%}$, respectively. Average $NO_{x50\%}$ of Car-A was approximately 0.015 g/s, and it was lower than 0.0006 g/s for the other two gasoline cars in the test. Average $NO_{x50\%}$ of the diesel passenger car was approximately 0.0035 g/s. Average $t_{50\%}$ of the four cars corresponding to $NO_{x50\%}$ was smaller than 13%. Car-B presented the highest mean value; average $t_{50\%}$ was approximately 3% for Car-A and Car-D. $t_{50\%}$ of a diesel passenger car corresponding to $NO_{x50\%}$ was approximately 7.3% and 3.7% respectively for LNT and SCR scenarios (Mera et al., 2019). It implied that the focus of NO_x reduction should not only be the cold start stages but also high emission peaks which were greatly affected by the driving behaviors. NO_x emission factors under dynamic conditions such as higher power output caused by large road grade were even high than real-driving emission (RDE) which fulfilled RDE boundary conditions (Suarez-Bertoa et al., 2019b), which addressed the importance of engine load to NO_x emissions. NO_x as the function of road grade was also fitted by a second order polynomial law, with NO_x emission factors increasing five times when the road grade was increased from zero to five (Costagliola et al., 2018).

Vehicle acceleration is considered to be the most important factor leading to high NO_x emission peaks. Fig. 7 shows $a_{NOx20\%}$, $a_{NOx50\%}$, and corresponding $t_{20\%}$ and $t_{50\%}$ of the four passenger cars. $a_{NOx20\%}$ presented a reverse tendency to corresponding $t_{20\%}$ for the four passenger cars. Average $a_{NOx20\%}$ was in the range of 0.6 m/s^2~ 1.35 m/s^2, with corresponding $t_{20\%}$ being in the range of 2~11%. The variations of $a_{NOx20\%}$ in the report (Mera et al., 2019) were much higher than the authors' results, with the maximum value being approximately 2.3 m/s^2; however, the average value was lower than the authors' results, being approximately 0.8 m/s^2. Average $a_{NOx20\%}$ was the highest and corresponding $t_{20\%}$ was the lowest for Car-D among the four cars. It implied that NO_x emissions of the diesel car (Car-D) were more sensitive to acceleration than the other cars. $a_{NOx20\%}$ had the smallest value and corresponding $t_{20\%}$ was the highest for Car-B. It was noted that fewer NO_x emission peaks were observed in the large acceleration process for Car-B; NO_x emissions of Car-B were less dependent on the acceleration than the other cars. The differences of average $a_{NOx20\%}$ were small for the three gasoline cars.

It was proved that NO_x emission factors of a diesel car under normal driving conditions were approximately 1.5 times of aggressive driving conditions (Varella et al., 2019). It indicated the variations of the emissions factors over various driving behaviors even similar traffic

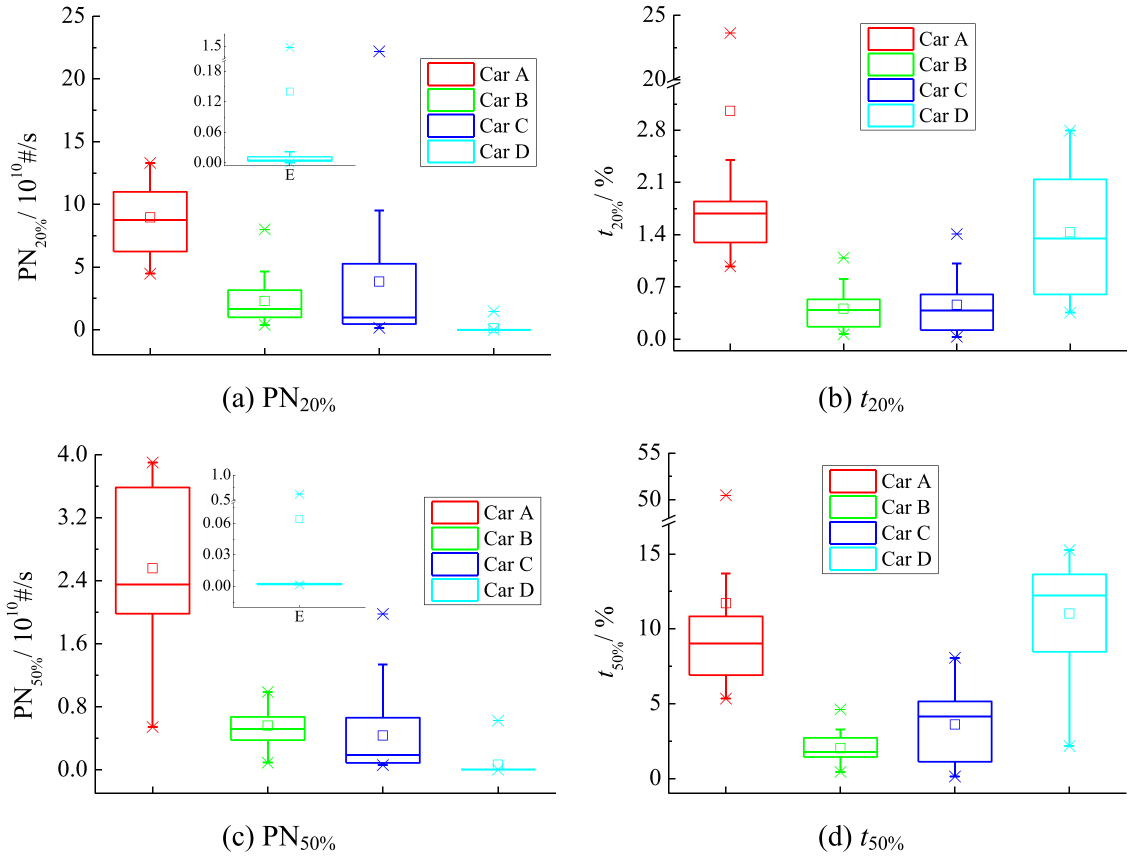

Fig. 9. PN emission rates and corresponding durations over 20% and 50% of the total PN emission.

conditions. Average $a_{NOx50\%}$ of Car-B approached to zero, and the corresponding $t_{50\%}$ was approximately 44%. It indicated that the deceleration process of Car-B also contributed a large proportion to total NO_x emissions; and the variations were low. Regarding Car-D, average $a_{NOx50\%}$ was still higher than 0.6 m/s^2 and corresponding $t_{50\%}$ was lower than 12%. Average $a_{NOx50\%}$ of a Euro-6b diesel car (Mera et al., 2019) was at the same level with the diesel car in this paper, being approximately 0.6 m/s^2. Distributions of NO_x emission rates were significantly unevenly dispersed. This finding was consistent with many previous studies (Ko et al., 2019; Mendoza-Villafuerte et al., 2017) where NO_x emission rates were quite low globally under real-world driving conditions as long as the engines were fully warmed up except for some aggressive driving events. Small variations of $a_{20\%}$ and $a_{50\%}$ indicated high tolerances of the passenger cars to the driving behavior variations, contributing to dropping high emission peaks.

The average speed and corresponding durations of 20% and 50% of the total NO_x emissions are shown in Fig. 8. The average $v_{NOx20\%}$ was in the range of 45 km/h~58 km/h; the corresponding $t_{20\%}$ ranged from 17% to 31%. It seemed that the NO_x emissions were relatively evenly distributed against speed. NO_x emissions were less dependent on the speed than the acceleration, concluding from the comparisons of Figs. 7 and 8. The differences of average $v_{NOx20\%}$ among Euro-6c and Euro-6d passenger cars were minor. Regarding Euro-6c and Euro-6d passenger cars, NO_x emissions under high speed conditions were lower than the average level because $t_{20\%}$ corresponding to $v_{NOx20\%}$ was higher than 20%. Average $v_{NOx50\%}$ was in the range of 27 km/h~ 41 km/h, with the corresponding $t_{50\%}$ being higher than 50% except for Car-A. It meant that much NO_x were generated under low speed conditions where the exhaust temperature was too low to ensure high NO_x removal efficiency of SCR system. Average $t_{50\%}$ corresponding to $v_{NOx50\%}$ was approximately 73% for Car-B, indicating the NO_x emissions were dominated by low speed operations. Higher speed of the cars was demonstrated to have higher variations of NO_x emission factors (Zhai et al., 2020), contributing to more emission peaks.

3.3. Variations of PN related KPIs

Euro-6 emission standard limits both PM and PN emissions for direct gasoline injection passenger cars and diesel passenger cars. DPF and GPF are effective to reduce PM emission; however, PN emission is still a challenge because of the low removal efficiency of DPF and GPF to ultrafine particles. Fig. 9 shows $PN_{20\%}$, $PN_{50\%}$, and corresponding durations over 20% and 50% of the total PN emission. Average $PN_{20\%}$ was the lowest and the variations were the smallest for the diesel passenger car (Car-D). Average $t_{20\%}$ corresponding to $PN_{20\%}$ was smaller than 3%, indicating the PN emission peaks were much higher than normal values. Meantime, average $t_{20\%}$ corresponding to $PN_{20\%}$ for Car-B and Car-C was smaller than 0.5%, showing that a small amount of vehicle operation points contributed 20% of the total PN emissions. These points should be the main regimes where the improvement should be done to drop PN emission from the viewpoint of driving behaviors. Additionally, more focus should be paid to PN emission peaks from direct injection gasoline cars even the cars had GPF systems. Variations of $t_{20\%}$ and $t_{50\%}$ for PN emission were higher than those of NO_x emissions. PN emission peaks were more sensitive to driving behaviors than NO_x emissions. The results were consistent with the published work (Suarez-Bertoa et al., 2019a) where the variations of the PN emission factors over real-world driving were in the range of 7×10^8#/km ~10^{11}#/km for Euro-6 passenger cars. The variations of PN emission factors were higher than those of NO_x emission factors (10 mg/ km ~600 mg/ km).

As demonstrated in the work (Tan et al., 2017), the particle removal efficiency was different for particles with different sizes. PN emission peaks were dependent on the particle size distributions to some extent. It was pointed out that high PN emission peaks over aggressive driving

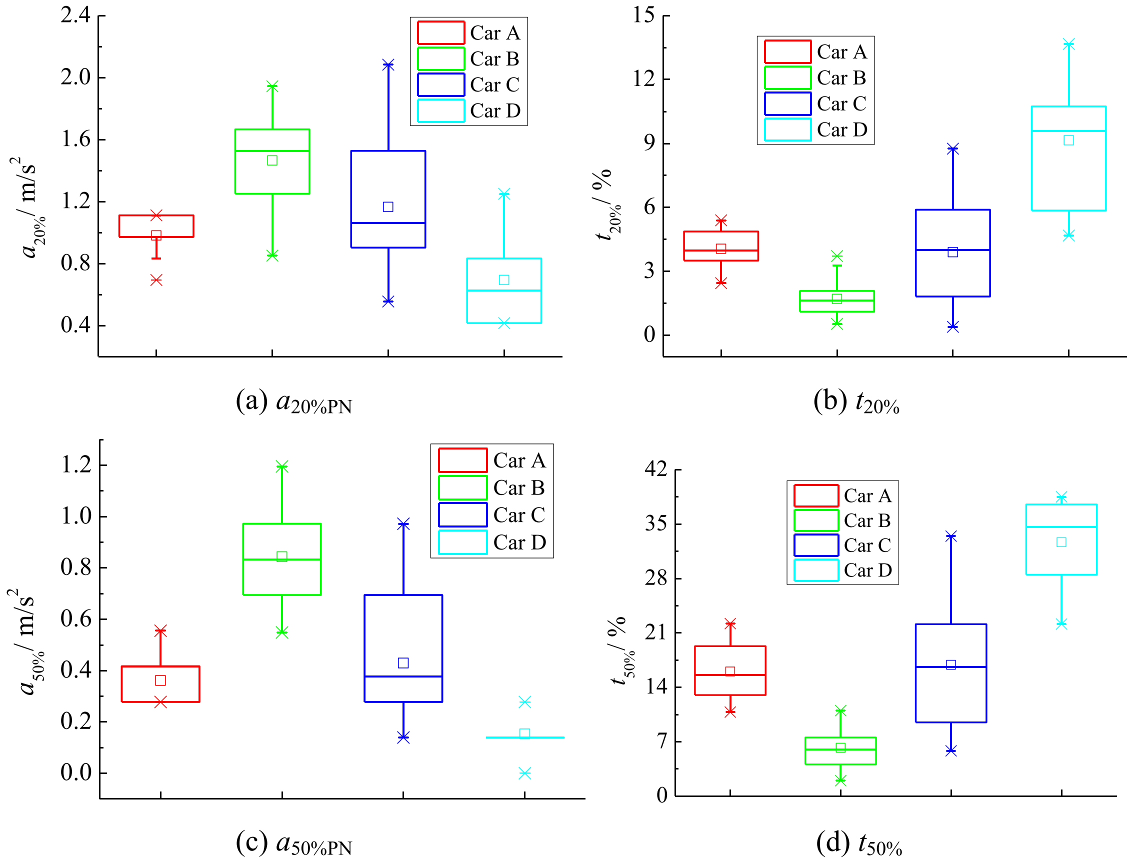

Fig. 10. Acceleration and corresponding durations over 20% and 50% of the total PN emission.

were hundreds times higher than those of normal driving conditions (Mendoza-Villafuerte et al., 2017). Particle emissions included both solid-phase and liquid-phase particles (Liu et al., 2010; Meloni and Palma, 2020). Solid-phase particle formations were mainly determined by in-cylinder combustion characteristics; liquid-phase particles were affected by both in-cylinder combustion and tailpipe temperature evolutions. Low temperature in tailpipes contributed to the formations of secondary liquid-phase particles. Part of the gaseous HC was condensed into liquid-phase particles which may be counted by PEMS (Casati et al., 2007; Liu et al., 2010; Meloni and Palma, 2020). PN emission factors of a diesel car under −15 °C ambient temperature was demonstrated to be 2.3 times higher than those under 5 °C ambient temperature (Lotfi, 2021). It indicated the significant contributions of gas-phase particles to total PN emission. It explained the reasons of the low values of $\mathrm{PN}_{20\%}$ and $\mathrm{PN}_{50\%}$ in this paper.

PN emission formations were significantly dependent on in-cylinder combustion temperature which was really high in the vehicle acceleration process due to much fuel delivery. The acceleration process not only affected solid-phase particle formations but also the liquid-phase particles. Additionally, liquid-phase particle size was usually smaller than solid-phase particles. Fig. 10 shows the car acceleration and corresponding durations over 20% and 50% of the total PN emission. Average $a_{\mathrm{PN}20\%}$ differed greatly among the four passenger cars, being in the range of 0.6 m/s^2~1.4 m/s^2, and the corresponding $t_{20\%}$ ranged from 1.5% to 10% for the given passenger cars. $a_{\mathrm{PN}20\%}$ was the highest for Car-B and the lowest for Car-D. It was inconsistent with the tendency of NO_x emissions. PN emission of the diesel passenger car (Car-D) was less sensitive to the acceleration than the other three passenger cars; it was the most sensitive for Car-B. It seemed the emissions of low emission cars were more dependent on the acceleration. High PN emission rates not only happened in high acceleration process but also normal driving conditions, especially for the diesel passenger car (Car-D) whose $a_{20\%}$ was approximately 0.75 m/s^2. Average $a_{\mathrm{PN}50\%}$ tendency was consistent with $a_{\mathrm{PN}20\%}$ for the four passenger cars. Average $t_{50\%}$ was in the range of 6~32%. The variations of PN emission factors under no GPF scenarios were at the same level as the ones with GPF (Demuynck et al., 2017), which was inconsistent with the authors' results. Additionally, the emission factors were close to the emission limits (Demuynck et al., 2017); however, they were far from the emission limits for the authors' results due to the exclusion of the liquid-phase PN emission during the test.

Variations of $v_{\mathrm{PN}20\%}$, $v_{\mathrm{PN}50\%}$ and corresponding $t_{20\%}$ and $t_{50\%}$ are presented in Fig. 11. The average $v_{\mathrm{PN}20\%}$ was in the range of 53 km/h~73 km/h, and the differences among the four cars were large. Variations of $v_{20\%}$ and corresponding $t_{20\%}$ for Car-B were much bigger than the other three passenger cars; $t_{20\%}$ was in the range of 7~22%. Car-C showed the highest value of average $v_{\mathrm{PN}20\%}$ and the lowest value of corresponding average $t_{20\%}$. It implied that PN emission factors of Car-C were sensitive to high speed regimes. $v_{\mathrm{PN}50\%}$ of the four passenger cars was in the range of 33 km/h~50 km/h, and corresponding $t_{50\%}$ ranged from 30% to 62%. It meant the PN emission factors were less sensitive to speed than acceleration for the given passenger cars. It was presented by the research (Yang et al., 2021), the PN emission factors did not have much difference when the speed was lower than 70 km/h. It explained the trend in Fig. 11 where the percentage of total travel time was close to the corresponding percentage of total emissions. It was proved that the variations of PN emission factors tended to be high under high speed and acceleration conditions.

4. Conclusions

NO_x and PN emissions of three Euro-6 compliant gasoline cars and a Euro-6 diesel car are monitored using PEMS during real-world driving with nineteen drivers. Specific contribution regimes of NO_x and PN

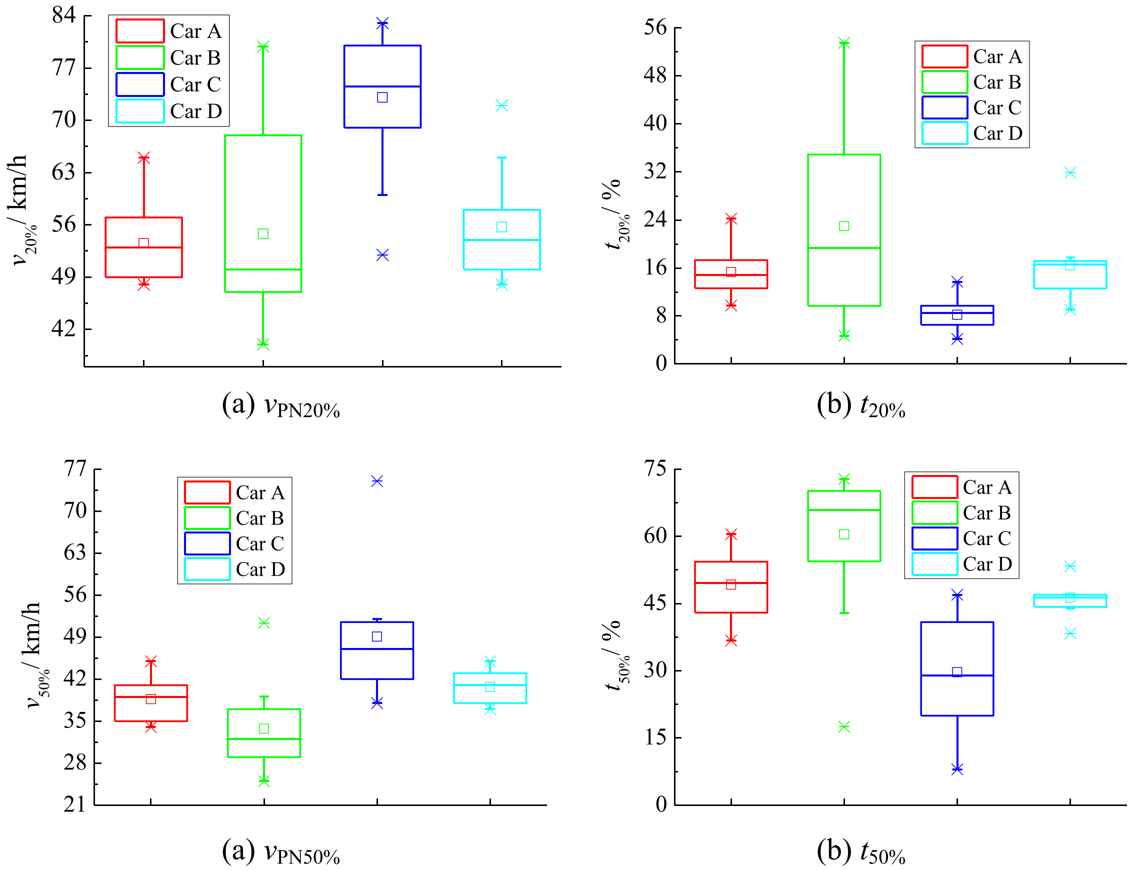

Fig. 11. Vehicle speed and corresponding durations over 50% of the total PN emission.

emissions to total emissions are analyzed using the authors' defined KPIs. The main contribution of this research is figuring out the main regimes where the NO_x and PN emissions may be dropped by improving driving behaviors (e.g. speed and acceleration). Additionally, the variations of the regimes over different drivers and cars are obtained. The main conclusions of this paper are as the follows:

1. The given Euro-6a gasoline car had much higher average NO_x and PN emission factors than the other three given passenger cars over the nineteen drivers, partly caused by different type approval driving cycles used in the emission regulations and being free of GPF. NO_x emission factors of the given diesel car (Euro-6d) were higher than the given Euro-6c and Euro-6d gasoline cars over the given test route and drivers; however, PN emission factors of the diesel car were much lower although the Euro-6d gasoline cars had GPFs. The ratios of NO_x and PN emissions at real-world driving to standard driving cycle were 2.29 and 1.65 for Car-A, respectively; additionally, the ratio was 3.22 for PN emissions from Car-D.

2. Average $NO_{x20\%}$ and $NO_{x50\%}$ presented the same pattern for the four passenger cars, and they were consistent with the tendency of average NO_x emission factors. The given passenger cars having lower average NO_x emission factors had lower variations of $NO_{x20\%}$ and $NO_{x50\%}$. High emission peaks in the real-world driving presented a great contribution to total emissions for the Euro-6a gasoline car and the diesel car whose $t_{20\%}$ corresponding to $NO_{x20\%}$ was lower than 1%.

3. Average $a_{NOx20\%}$ of the diesel car was the highest, and the corresponding $t_{20\%}$ was the lowest among the four passenger cars. NO_x emission factors of the given diesel car were much more dependent on the acceleration than the three given gasoline cars over the specific test route and drivers. Average $t_{20\%}$ corresponding to $v_{NOx20\%}$ was in the range of 10~30%. NO_x emission factors were less sensitive to vehicle speed than acceleration.

4. The trend of average $PN_{20\%}$ and $PN_{50\%}$ by car types were consistent with PN emission factors. PN emission peaks had really high contributions to total PN emission because average $t_{20\%}$ corresponding to $PN_{20\%}$ was lower than 2% for all the four given passenger cars. The average $t_{20\%}$ corresponding to $a_{PN20\%}$ was the lowest for the Euro-6d gasoline car and it was the highest for the diesel car. Euro-6d gasoline car (Car-C) was the most sensitive to vehicle acceleration in terms of PN emission, and the diesel car (Car-D) was the least sensitive to the acceleration. PN emission of the passenger cars depended more on vehicle acceleration than speed.

5. In order to further drop NO_x emissions from the viewpoint of improving driving behaviors, the acceleration of the drivers over the three given gasoline car was suggested to be smaller than 0.8 m/s^2 and it should be smaller than 1.3 m/s^2 for the given diesel car. Regarding low PN emission driving, acceleration was recommended to be lower than 1.0 m/s^2 for the three given gasoline car, and it should be smaller than 0.6 m/s^2 for the given diesel car if possible.

CRediT authorship contribution statement

Jianbing Gao: Formal analysis, Investigation, Methodology, Resources, Validation, Visualization, Writing – original draft, Writing – review & editing. **Yufeng Wang**, **Haibo Chen:** Conceptualization, Funding acquisition, Methodology, Project administration, Resources, Software, Supervision, Visualization, Writing – review & editing. **Ye Liu:** Investigation, Writing – review & editing. **Juhani Laurikko:** Data collection. **Ying Li:** Visualization, Writing – review & editing.

Declaration of Competing Interest

The authors declare that they have no known competing financial interests or personal relationships that could have appeared to influence the work reported in this paper.

Acknowledgement

The research reported in this paper was supported by the EU-funded project Modify drivers' behaviour to adapt for lower emissions (grant agreement No 815189).

Appendix A. Supporting information

Supplementary data associated with this article can be found in the online version at doi:10.1016/j.jhazmat.2021.127590.

References

Carslaw, D.C., Beevers, S.D., Tate, J.E., Westmoreland, E.J., Williams, M.L., 2011. Recent evidence concerning higher NOx emissions from passenger cars and light duty vehicles. Atmos. Environ. 45 (39), 7053–7063.

Casati, R., Scheer, V., Vogt, R., Benter, T., 2007. Measurement of nucleation and soot mode particle emission from a diesel passenger car in real world and laboratory in situ dilution. Atmos. Environ. 41 (10), 2125–2135.

Costagliola, M.A., Costabile, M., Prati, M.V., 2018. Impact of road grade on real driving emissions from two Euro 5 diesel vehicles. Appl. Energy 231, 586–593.

Degraeuwe, B., Weiss, M., 2017. Does the new European driving cycle (NEDC) really fail to capture the NOX emissions of diesel cars in Europe? Environ. Pollut. 222, 234–241.

Demuynck, J., Favre, C., Bosteels, D., Hamje, H., Andersson, J., 2017. Real-world emissions measurements of a gasoline direct injection vehicle without and with a gasoline particulate filter. SAE Technical Paper.

Drozd, G.T., Zhao, Y., Saliba, G., Frodin, B., Maddox, C., Oliver Chang, M.-C., Maldonado, H., Sardar, S., Weber, R.J., Robinson, A.L., 2018. Detailed speciation of intermediate volatility and semivolatile organic compound emissions from gasoline vehicles: Effects of cold-starts and implications for secondary organic aerosol formation. Environ. Sci. Technol. 53 (3), 1706–1714.

Fontaras, G., Karavalakis, G., Kousoulidou, M., Tzamkiozis, T., Ntziachristos, L., Bakeas, E., Stournas, S., Samaras, Z., 2009. Effects of biodiesel on passenger car fuel consumption, regulated and non-regulated pollutant emissions over legislated and real-world driving cycles. Fuel 88 (9), 1608–1617.

Gao, J., Chen, H., Liu, Y., Laurikko, J., Li, Y., Li, T., Tu, R., 2021a. Comparison of NOx and PN emissions between Euro 6 petrol and diesel passenger cars under real-world driving conditions. Sci. Total. Environ., 149789

Gao, J., Chen, H., Liu, Y., Ying, L., Li, T., Tu, R., Liang, B., Ma, C., 2021b. The effect of after-treatment techniques on the correlations between driving behaviours and NOx emissions of a passenger cars. J. Clean. Prod. 288, 125647.

Gao, J., Tian, G., Sorniotti, A., 2019a. On the emission reduction through the application of an electrically heated catalyst to a diesel vehicle. Energy Sci. Eng. 7 (6), 2383–2397.

Gao, J., Tian, G., Sorniotti, A., Karci, A.E., Di Palo, R., 2019b. Review of thermal management of catalytic converters to decrease engine emissions during cold start and warm up. Appl. Therm. Eng. 147, 177–187.

Gao, J., Wang, X., Song, P., Tian, G., Ma, C., 2022. Review of the backfire occurrences and control strategies for port hydrogen injection internal combustion engines. Fuel 307, 121553.

Guan, B., Zhan, R., Lin, H., Huang, Z., 2015. Review of the state-of-the-art of exhaust particulate filter technology in internal combustion engines. J. Environ. Manag. 154, 225–258.

Hu, J., Wu, Y., Wang, Z., Li, Z., Zhou, Y., Wang, H., Bao, X., Hao, J., 2012. Real-world fuel efficiency and exhaust emissions of light-duty diesel vehicles and their correlation with road conditions. J. Environ. Sci. 24 (5), 865–874.

Huang, C., Lou, D., Hu, Z., Feng, Q., Chen, Y., Chen, C., Tan, P., Yao, D., 2013. A PEMS study of the emissions of gaseous pollutants and ultrafine particles from gasoline-and diesel-fueled vehicles. Atmos. Environ. 77, 703–710.

G. Kadijk, G., van Mensch, P., Ligterink, N.E.J.Jo.E.S., 2017. Engineering. Var. Real. World NOx Emiss. Diesel Eur. 5 6 Light-duty Veh., 7, 1, pp. 11–32.

Ko, J., Myung, C.-L., Park, S., 2019. Impacts of ambient temperature, DPF regeneration, and traffic congestion on NOx emissions from a Euro 6-compliant diesel vehicle equipped with an LNT under real-world driving conditions. Atmos. Environ. 200, 1–14.

Kontses, A., Triantafyllopoulos, G., Ntziachristos, L., Samaras, Z., 2020. Particle number (PN) emissions from gasoline, diesel, LPG, CNG and hybrid-electric light-duty vehicles under real-world driving conditions. Atmos. Environ. 222, 117126.

Li, M., 2019. A Complete Guide to Box Plots. Chartio-Data Tutorials.

Liu, H., Yu, Y., Wang, C., Xu, H., Ma, X., 2021. Brownian coagulation of particles in the gasoline engine exhaust system: experimental measurement and Monte Carlo simulation. Fuel 303, 121340.

Liu, Z.G., Berg, D.R., Vasys, V.N., Dettmann, M.E., Zielinska, B., Schauer, J.J., 2010. Analysis of C1, C2, and C10 through C33 particle-phase and semi-volatile organic compound emissions from heavy-duty diesel engines. Atmos. Environ. 44 (8), 1108–1115.

Lotfi, A., 2021. Study Light-duty Gasol. Veh. cold Clim. NOx Part. Number Emiss. Real. -World Driv. Cond. 2021.

Luján, J.M., Bermúdez, V., Dolz, V., Monsalve-Serrano, J., 2018. An assessment of the real-world driving gaseous emissions from a Euro 6 light-duty diesel vehicle using a portable emissions measurement system (PEMS). Atmos. Environ. 174, 112–121.

Meloni, E., Palma, V., 2020. Most recent advances in diesel engine catalytic soot abatement: structured catalysts and alternative approaches. Catalysts 10 (7), 745.

Mendoza-Villafuerte, P., Suarez-Bertoa, R., Giechaskiel, B., Riccobono, F., Bulgheroni, C., Astorga, C., Perujo, A., 2017. NOx, NH3, N2O and PN real driving emissions from a Euro VI heavy-duty vehicle. Impact of regulatory on-road test conditions on emissions. Sci. Total Environ. 609, 546–555.

Mera, Z., Fonseca, N., López, J.-M., Casanova, J., 2019. Analysis of the high instantaneous NOx emissions from Euro 6 diesel passenger cars under real driving conditions. Appl. Energy 242, 1074–1089.

Merkisz, J., Bielaczyc, P., Pielecha, J., Woodburn, J., 2019. RDE testing of passenger cars: The effect of the cold start on the emissions results. SAE Technical Paper.

Myung, C.-L., Choi, K., Cho, J., Kim, K., Baek, S., Lim, Y., Park, S., 2020. Evaluation of regulated, particulate, and BTEX emissions inventories from a gasoline direct injection passenger car with various ethanol blended fuels under urban and rural driving cycles in Korea. Fuel 262, 116406.

Nagpure, A.S., Gurjar, B., Kumar, V., Kumar, P., 2016. Estimation of exhaust and non-exhaust gaseous, particulate matter and air toxics emissions from on-road vehicles in Delhi. Atmos. Enviorn. 127, 118–124.

O'Driscoll, R., Stettler, M.E., Molden, N., Oxley, T., ApSimon, H.M., 2018. Real world CO_2 and NOx emissions from 149 Euro 5 and 6 diesel, gasoline and hybrid passenger cars. Sci. Total Environ. 621, 282–290.

Pathak, S.K., Sood, V., Singh, Y., Channiwala, S., 2016. Real world vehicle emissions: their correlation with driving parameters. Transp. Res. Part D: Transp. Environ. 44, 157–176.

Penconek, A., Drążyk, P., Moskal, A., 2013. Penetration of diesel exhaust particles through commercially available dust half masks. Ann. Occup. Hyg. 57 (3), 360–373.

Ramos, A., Muñoz, J., Andrés, F., Armas, O., 2018. NOx emissions from diesel light duty vehicle tested under NEDC and real-word driving conditions. Transp. Res. Part D: Transp. Environ. 63, 37–48.

Suarez-Bertoa, R., Kousoulidou, M., Clairotte, M., Giechaskiel, B., Nuottimäki, J., Sarjovaara, T., Lonza, L.J.F., 2019a. Impact HVO blends Mod. Diesel Passeng. cars Emiss. Real. World Oper. 235, pp. 1427–1435.

Suarez-Bertoa, R., Valverde, V., Clairotte, M., Pavlovic, J., Giechaskiel, B., Franco, V., Kregar, Z., Astorga, C., 2019b. On-road emissions of passenger cars beyond the boundary conditions of the real-driving emissions test. Environ. Res. 176, 108572.

Tan, P.-q, Zhong, Y.-m, Hu, Z.-y, Lou, D.-m, 2017. Size distributions, PAHs and inorganic ions of exhaust particles from a heavy duty diesel engine using B20 biodiesel with different exhaust aftertreatments. Energy 141, 898–906.

The UK Government, T.U.G., 2021. Emissions of air pollutants in the UK.

Tong, R., Liu, J., Wang, W., Fang, Y., 2020. Health effects of PM2. 5 emissions from on-road vehicles during weekdays and weekends in Beijing, China. Atmos. Enviorn. 223, 117258.

Triantafyllopoulos, G., Dimaratos, A., Ntziachristos, L., Bernard, Y., Dornoff, J., Samaras, Z., 2019. A study on the CO_2 and NOx emissions performance of Euro 6 diesel vehicles under various chassis dynamometer and on-road conditions including latest regulatory provisions. Sci. Total Environ. 666, 337–346.

Valverde, V., Mora, B.A., Clairotte, M., Pavlovic, J., Suarez-Bertoa, R., Giechaskiel, B., Astorga-LLorens, C., Fontaras, G., 2019. Emission factors derived from 13 Euro 6b light-duty vehicles based on laboratory and on-road measurements. Atmos. Environ. 10 (5), 243.

Varella, R.A., Faria, M.V., Mendoza-Villafuerte, P., Baptista, P.C., Sousa, L., Duarte, G.O., 2019. Assessing the influence of boundary conditions, driving behavior and data analysis methods on real driving CO_2 and NOx emissions. Sci. Total Enviorn. 658, 879–894.

Wang, Jeong, Zimmerman, C.-H., Healy, N., Hilker, R., Evans, N., 2017a. Real-world emission of particles from vehicles: volatility and the effects of ambient temperature. Environ. Sci. Technol 4081–4090.

Wang, Quiros, Thiruvengadam, D.C., Pradhan, A., Hu, S., Huai, S., Lee, T., Zhu, E.S., 2017b. Total particle number emissions from modern diesel, natural gas, and hybrid heavy-duty vehicles during on-road operation. Environ. Sci. Technol. 51 (12), 6990–6998.

Wang, Y., Hao, C., Ge, Y., Hao, L., Tan, J., Wang, X., Zhang, P., Wang, Y., Tian, W., Lin, Z., 2020. Fuel consumption and emission performance from light-duty conventional/hybrid-electric vehicles over different cycles and real driving tests. Fuel 278, 118340.

Weber, C., Sundvor, I., Figenbaum, E., 2019. Comparison of regulated emission factors of Euro 6 LDV in Nordic temperatures and cold start conditions: diesel-and gasoline direct-injection. Atmos. Environ. 206, 208–217.

Wu, Y., Zhang, S., Hao, J., Liu, H., Wu, X., Hu, J., Walsh, M.P., Wallington, T.J., Zhang, K.M., Stevanovic, S., 2017. On-road vehicle emissions and their control in China: a review and outlook. Sci. Total Environ. 574, 332–349.

Yang, Z., Zhang, X., Xie, Z., Qi, S., Wang, J., Li, J., Li, M., 2021. Research on the characteristics of real-world vehicle particle number and mass emissions, IOP Conference Series: Earth and Environmental Science. IOP Publishing, p. 012013.

Yinhui, W., Rong, Z., Yanhong, Q., Jianfei, P., Mengren, L., Jianrong, L., Yusheng, W., Min, H., Shijin, S., 2016. The impact of fuel compositions on the particulate emissions of direct injection gasoline engine. Fuel 166, 543–552.

Zhai, Z., Tu, R., Xu, J., Wang, A., Hatzopoulou, M.J.A., 2020. Capturing Var. Instant. Veh. Emiss. Based Field Test. data, 11, 7, 765.

Zhang, M., Ge, Y., Wang, X., Tan, J., Hao, L., Xu, H.J.F., 2021. Part. Emiss. Direct-Inject. Comb. -Inject. Veh. fueled Gasol. /ethanol match-blends–Effects ethanol Aromat. Compos., 302, 121010.